3D RTM angle gathers from source wave propagation direction and dip of reflector

Kwangjin Yoon, Manhong Guo, Jun Cai and Bin Wang, TGS*

Summary

Creating an angle gather is a conceptually simple process of plotting reflection amplitudes along the angle. Reflection or opening angle can be directly calculated from source and receiver wave propagation directions or source propagation direction and dip of the reflector. We studied a cost effective approach to generate 3D Reverse Time Migration (RTM) angle gathers from source wave propagation direction and dip information. This is a mapping process of the shot image onto an angle and azimuth plane using the most energetic arrivals and their amplitudes and propagation directions.

Introduction

Sava and Fomel (2003) proposed a method to generate angle gathers in wave equation shot profile migration. This method converts Offset Domain Common Image Gather (ODCIG) to Angle Domain Common Image Gather (ADCIG). Fomel (2004) extended this approach to 3D. This approach causes artifacts in angle gathers due to the Fourier Transform. Xu et al. (2011) derived another approach for RTM 3D angle gathers using wavenumber domain convolution of the source and receiver wavefields and a more accurate Fourier transform method. However, this method demands intensive computations.

RTM angle gathers can be efficiently produced using the source wave propagation directions and the dips of the reflectors which can be estimated from the stack image of shot profiles (Zhang and McMechan, 2011). Yoon and Marfurt (2006) showed that the propagation direction of the dominant wave can be calculated using the Poynting vector. In RTM, if we store the snapshots and Poynting vectors on the disk, most energetic wavefields and corresponding propagation directions can be picked by scanning the snapshots and Poynting vectors. RTM Angle gathers can be built up by mapping the RTM shot profile image to an angle and azimuth plane using Poynting vectors and dips of the reflectors. Both source and receiver side wavefields can be combined for angle and azimuth calculations. We used source side Poynting vectors because receiver side wavefields are complex and their propagation directions are not as much reliable as the source side propagation directions. However, receiver side Poynting vectors may be applied to the azimuth calculation.

This approach has the limitation that the azimuth is defined by the source side propagation direction. However, we can take advantages like as; (1) It is efficient. It affords dense angle gathers without huge memory and computations. (2) The artifact caused by conversion from ODCIG can be suppressed. (3) In case the dip field has been updated, it enables us to regenerate angle gathers with ease by redoing the mapping process. (4) It has no limitation in media. If RTM can be performed, we can generate angle gathers.

Method

In RTM, we carry out wavefield propagation modeling. Propagation directions of dominant wavefields can be calculated by Poynting vector (Yoon and Marfurt, 2006). The Poynting vector at a time step *t* is given as

$$\vec{p}(x,t) = -\dot{u}(x,t)\nabla u(x,t)\,, \qquad (1)$$

where $\vec{p}(x,t)$ is the Poynting vector, $\dot{u}(x,t) = du(x,t)/dt$, $\nabla u(x,t)$ is the gradient of $u(x,t)$ and $u(x,t)$ is the amplitude. Computation of the Poynting vector can be erroneous if the numerical derivatives in time and space are not accurate enough. $\nabla u(x,t)$ can afford a coarse grid of two or three grid points for the shortest wavelength using high-order finite difference or pseudo-spectral methods. We may stack the Poynting vector for some period to achieve stable results instead of using the high order approximation scheme for $\dot{u}(x,t)$. Figure 1 shows a source wave snapshot and its Poynting vectors which have been stacked over four periods of the highest frequency. The Poytning vector $\vec{p}(x,t)_{stack}$ stacked over four periods can be expressed as

$$\vec{p}(x,t)_{stack} = \sum_{\tau=t-2T}^{\tau=t+2T} W(\tau-t)\,\vec{p}(x,\tau)\,, \qquad (2)$$

where $T = 1/f_{cut}$, f_{cut} is the highest frequency of the source wavelet and $W(\tau-t)$ is a Gaussian weighting function. Poynting vectors were calculated at not every time step but each time step matching the time increment $1/(4f_{cut})$.

The RTM image can be expressed as

$$I(x) = \int_{t=0}^{t=t_{\max}} S(x,t)R(x,t)dt\,, \qquad (3)$$

where $S(x,t)$ and $R(x,t)$ are source and receiver side wavefields, respectively, and $t_{\max}$ is the recording time. Angle gathers can be composed directly from the Poytning vectors and reflector dips by mapping the cross correlation between source and receiver wavefields $S(t)R(t)$ to angles at each time step. However, at a subsurface point, source wavefields have only one dominant arrival in a single ray path area and at most a few dominant arrivals in multi-path areas. These dominant arrivals mainly contribute to the shot profile RTM image. Based on this observation, we can pick a few of the most energetic arrivals and perform mapping of the final RTM image $I(x)$ to angles after migration without significant loss of accuracy. Pictures in Figure 2 explain this approach. Figure 2(a) shows propagation directions of the three most energetic arrivals. The angle range is -180º (white) to 180º (black). Figure 2(b) shows normalized relative amplitudes of the three most energetic arrivals. Figure 2(c) and Figure 2(d) denote the shot profile RTM image and its angle gathers which were produced by mapping the shot image using the propagation directions and relative amplitudes of the three most energetic arrivals.

To stack Poynting vectors for some time interval, we need to store Poynting vectors on the disk. The disk usage and computations can be reduced by using a low frequency source wavelet. We applied 5 Hz Ricker wavelet for most energetic arrivals and Poynting vectors. Wave scattering phenomena are different at different frequency bands. However, the kinematic properties of major wavefields are consistent. We have not observed significant differences in most energetic arrival traveltimes and Poynting vectors at different source wavelet spectrums.

In wave propagation of band limited wavelet, two arrivals can't be separated if the traveltimes are close to each other because the period of the wavelet should be considered. We assume the period of source wavelet packet as the period of the peak frequency or the center frequency of source spectrum. The most energetic traveltime t_{m1} has been picked first by scanning the source side wavefields. After then, the second most energetic traveltime t_{m2} has been picked among the traveltimes outside of $t_{m1}-T\sim t_{m1}+T$, where T is the period of source wavelet. This most energetic traveltimes picking approach has the limitation that closely arriving events can't be handled. However, any event separated longer than the period can be picked with ease.

Examples

We applied the angle gather generation using source wave propagation direction and dip to 2D and 3D data sets. The angle gathers produced in this paper have the angle range of 0°~60°. Figure 3 shows 2D angle gathers produced from BP TTI RTM images using the exact parameters. Angle gathers in Figure 3(a) were converted from ODCIGs following Sava and Fomel (2003). Angle gathers in Figure 3(b) were produced by the approach proposed in this paper. Gathers in Figure 3(b) show higher signal to noise level and flatter events than the gathers in Figure 3(a). Differences between two approaches are distinguishable especially at top of salt and subsalt areas. Figure 3(b) shows clearer and flatter events in these areas. Figure 4 and Figure 5 are angle gathers generated from SEG/EAGE 3D narrow azimuth dataset. Figure 4(a), 4(b) and 4(c) are RTM image, angle gathers converted from ODCIGs and produced by our approach, respectively. Figure 5(a), 5(b) and 5(c) are enlarged version of Figure 4(b), 4(c) and multi azimuth angle gathers by our approach, respectively. The gathers in Figure 5(c) are plotted in three azimuths; -30°~30°, 30°~90° and 90°~150°. In Figure 4(c) and Figure 5(b) and 5(c), we can see the crossing and curving down events shown in Figure 4(b) and Figure 5(a) have been suppressed well. Finally, we tested this approach with a dataset composed of a few wide azimuth sequences before tomographic velocity update. Figure 6(a) shows angle gathers converted from ODCIGs. Figure 6(b) and 6(c) are corresponding single and multi-azimuth angle gathers produced by our approach. The gathers in Figure 6(c) are plotted in six azimuths; -15°~15°, 15°~45°, 45°~75°, 75°~105°, 105°~135°, and 135°~165°. In Figure 6(a), gathers are significantly contaminated by noise due to the small coverage of the dataset and show moveout curvatures due to the insufficient velocity update. In Figure 6(b) and 6(c), we can see that noisy crossing and curving down events have disappeared and the curvatures have been preserved well.

Conclusions

We studied 3D RTM subsurface angle gathers using source side wave propagation directions and dips of reflectors. This approach is cost-effective and straight forward. For a RTM shot profile image, angle gathers are produced by mapping the RTM image using tables of Poynting vectors and relative amplitudes of most energetic arrivals after RTM. Additional computation and disk usage can be reduced by using low frequency source wavelet. This approach has the drawback that the azimuth of angle gather is defined by source wave propagation direction. However, angle gathers studied in this paper give high signal to noise ratio especially complex areas. Although, our approach has the limitations that only a few most energetic events are used and closely arriving events can't be identified. The power of stacking looks to make such limitations acceptable.

Acknowledgements

We thank BP and SEG/EAGE for synthetic datasets and TGS for the permission of this paper.

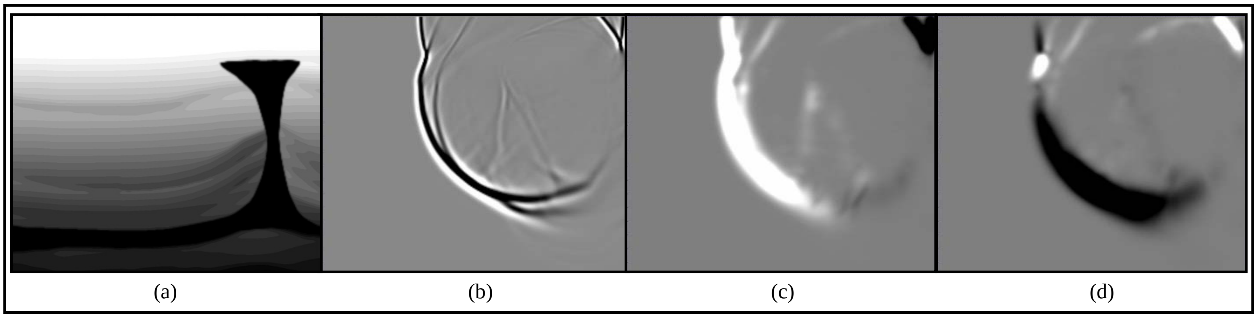

Figure 1. (a) 2D BP TTI velocity model, (b) snapshot of source wavefield and Poynting vectors (c) $p_x = -\dot{u}(du/dx)$, (d) $p_z = -\dot{u}(du/dz)$.

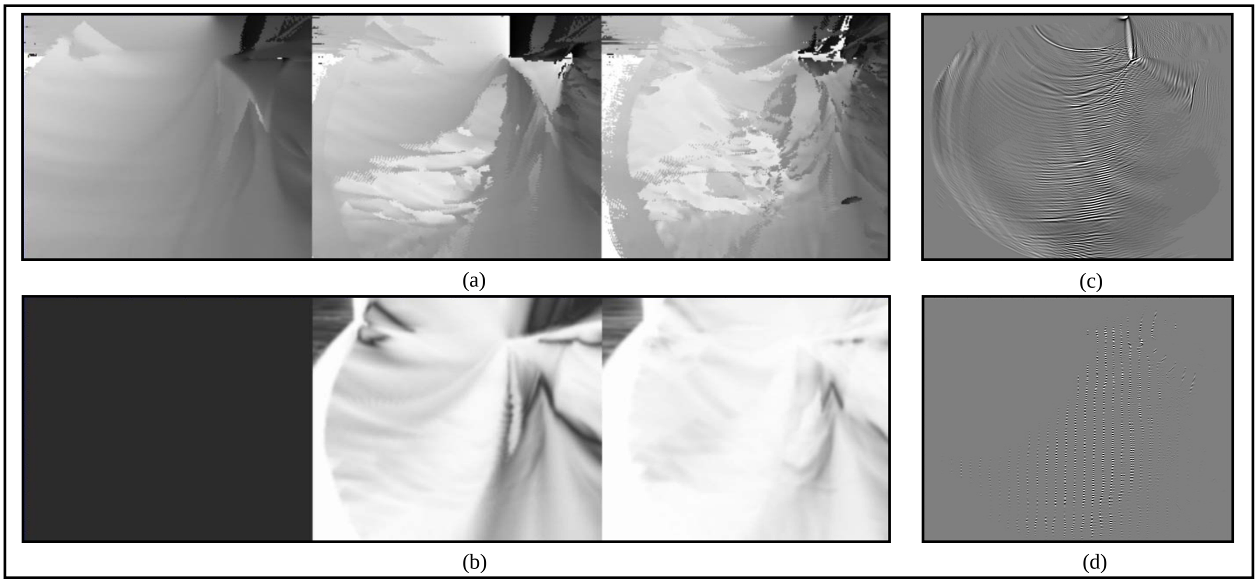

Figure 2. (a) Source wave propagation directions, (b) relative amplitudes of three most energetic arrivals, (c) RTM image and (d) angle gathers produced by mapping the RTM image using source wave propagation directions, dip and relative amplitudes.

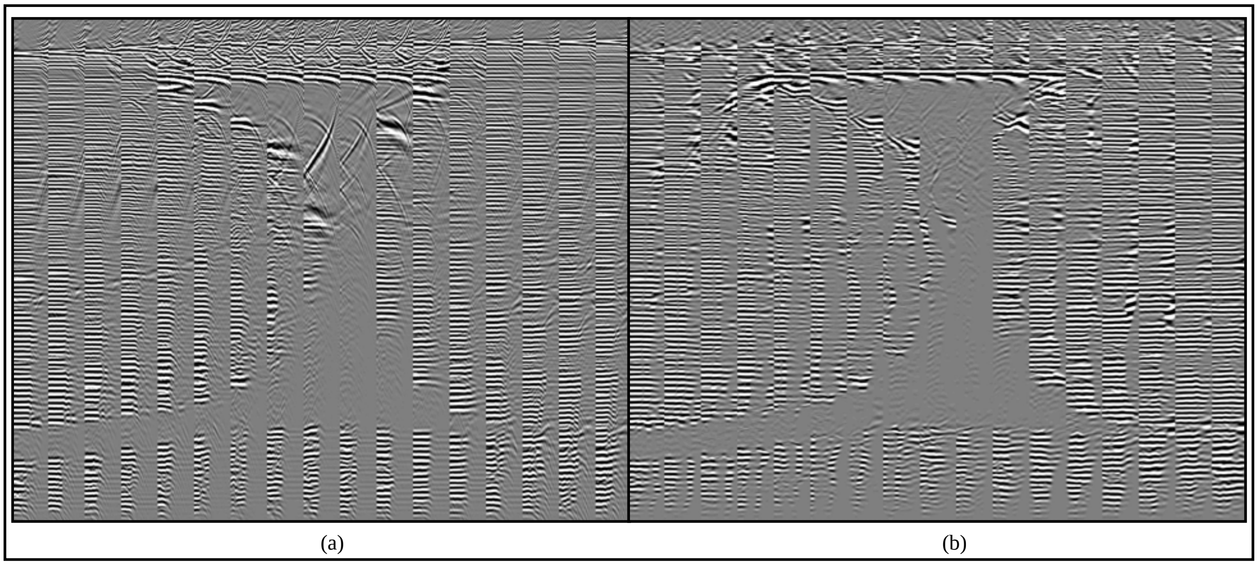

Figure 3. Angle gathers of 2D BP TTI dataset (a) converted from ODCIGs and (b) produced by the method studied in this paper.

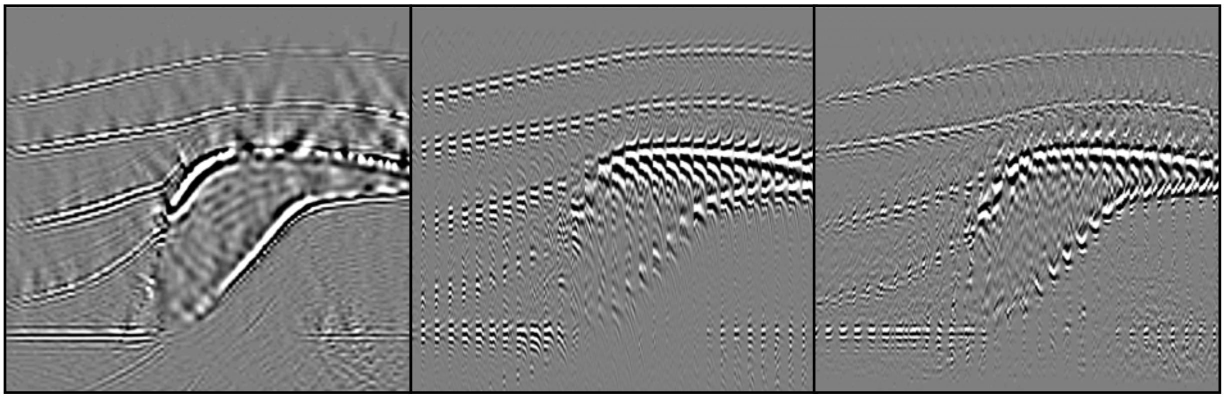

(a) (b) (c)

Figure 4. (a) RTM image, (b) angle gathers converted from ODCIGs and (c) angle gathers by the method studied in this paper of 3D SEG/EAGE narrow azimuth dataset.

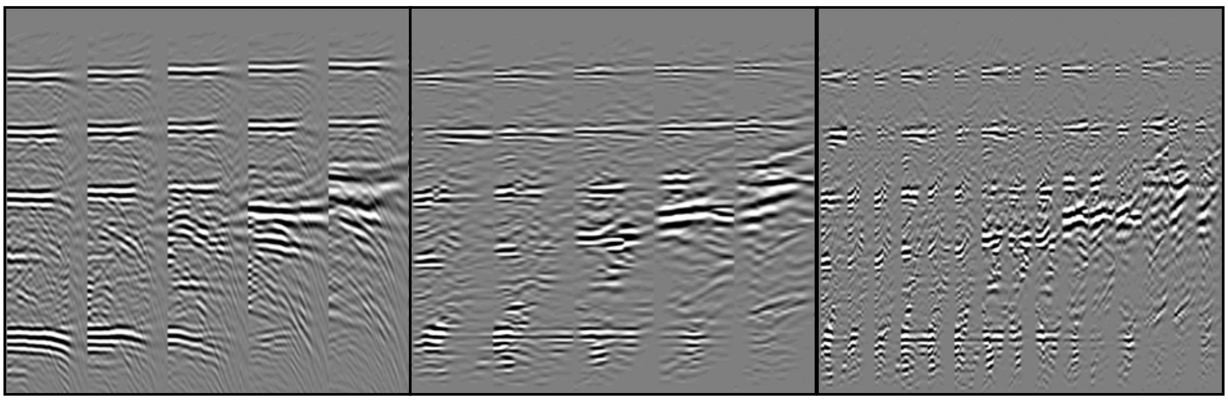

(a) (b) (c)

Figure 5. Enlarged versions of (a) Figure 4(b), (b) Figure 4(c) and (c) multi azimuth (-30°~30°, 30°~90° and 90°~150°) angle gathers by the method studied in this paper.

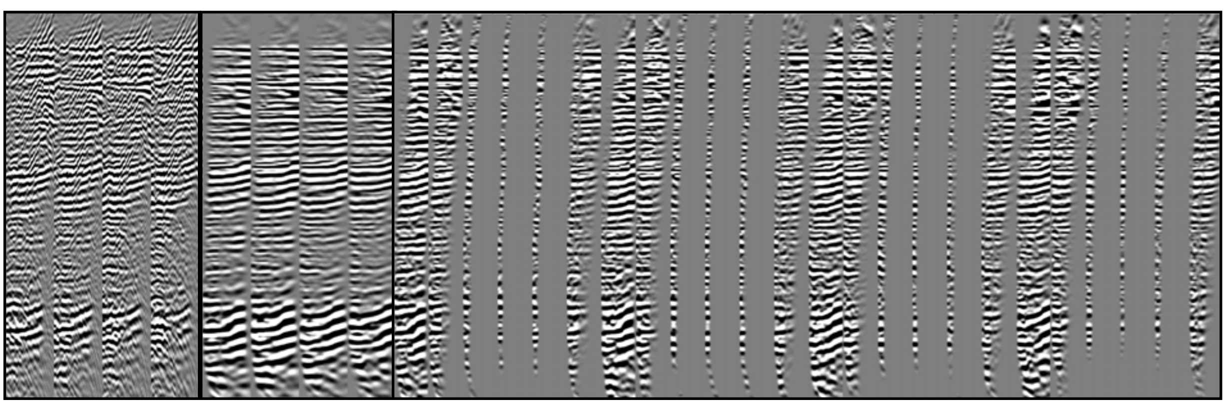

(a) (b) (c)

Figure 6. Angle gathers of a GOM wide azimuth dataset. (a) gathers converted from ODCIGs and (b) single and (c) multi azimuth gathers by the method studied in this paper.

EDITED REFERENCES

Note: This reference list is a copy-edited version of the reference list submitted by the author. Reference lists for the 2011 SEG Technical Program Expanded Abstracts have been copy edited so that references provided with the online metadata for each paper will achieve a high degree of linking to cited sources that appear on the Web.

REFERENCES

Fomel, S., 2004, Theory of 3D angle gathers in wave-equation imaging: 74thAnnual International Meeting, SEG, Expanded Abstracts, 1053–1056.

Sava, P., and S. Fomel, 2003, Angle-domain common-image gathers by wavefield continuation methods: Geophysics, **68**, 1065–1074, doi:10.1190/1.1581078.

Xu, S., Y. Zhang, and B. Tang, 2011, 3D angle gathers from reverse-time migration: Geophysics, **76**, no. 2, S77–S92, doi:10.1190/1.3536527.

Yoon, K., K. Marfurt, and W. Starr, 2004, Challenges in reverse-time migration: 74th Annual International Meeting, SEG, Expanded Abstracts, 1057–1060.

Zhang, Q., and G. McMechen, 2011, Angle-domain common-image gathers from reverse-time migrated images in isotropic and elastic media: Presented at the 81st Annual International Meeting, SEG.